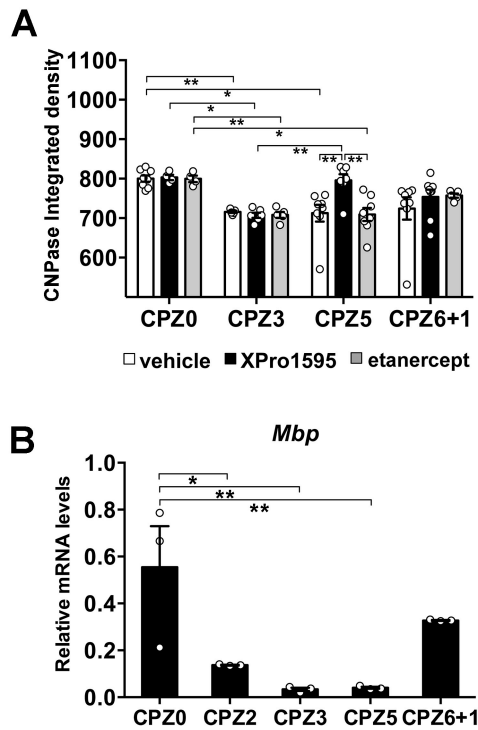
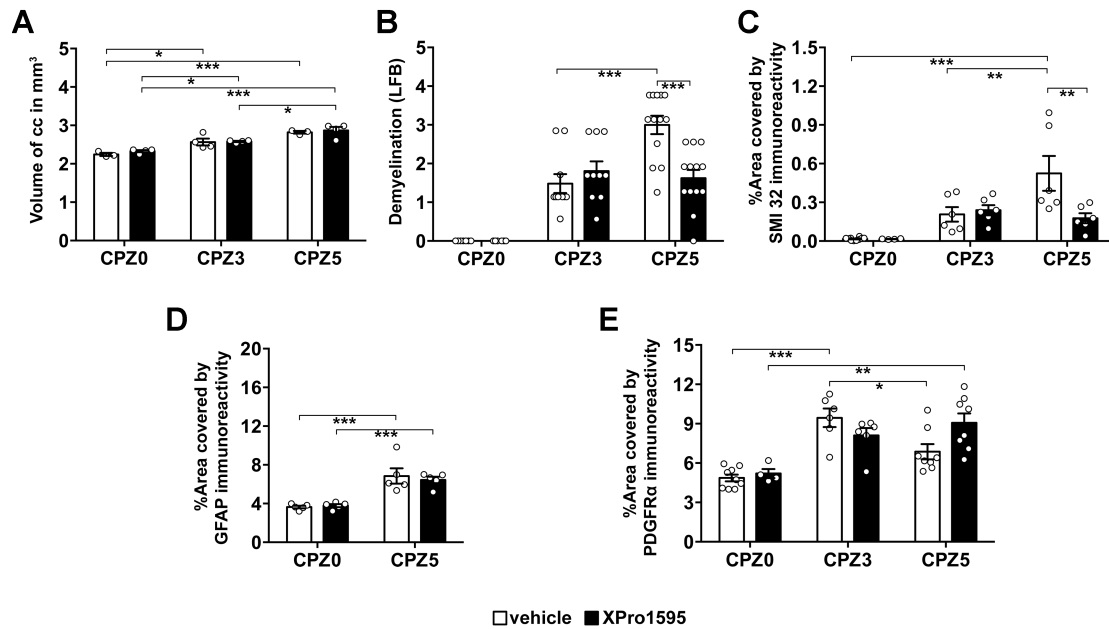


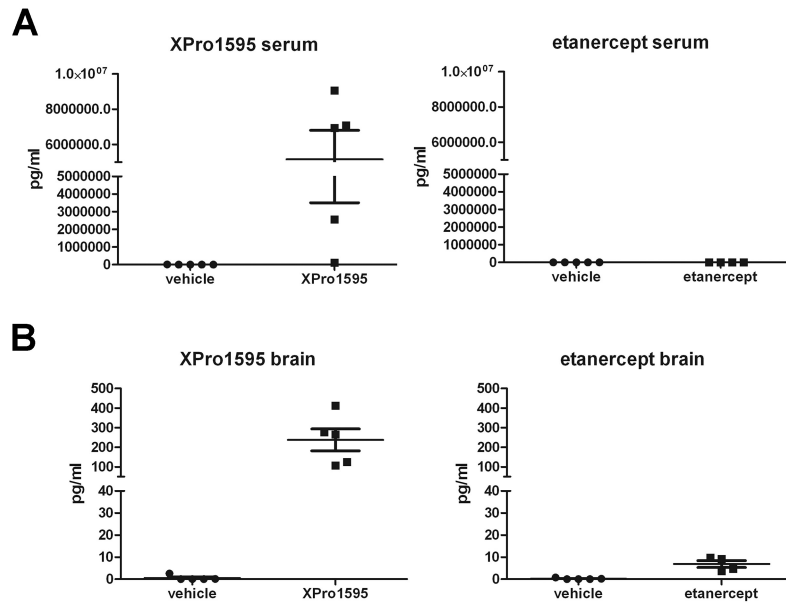
Supplementary Figures and Legends



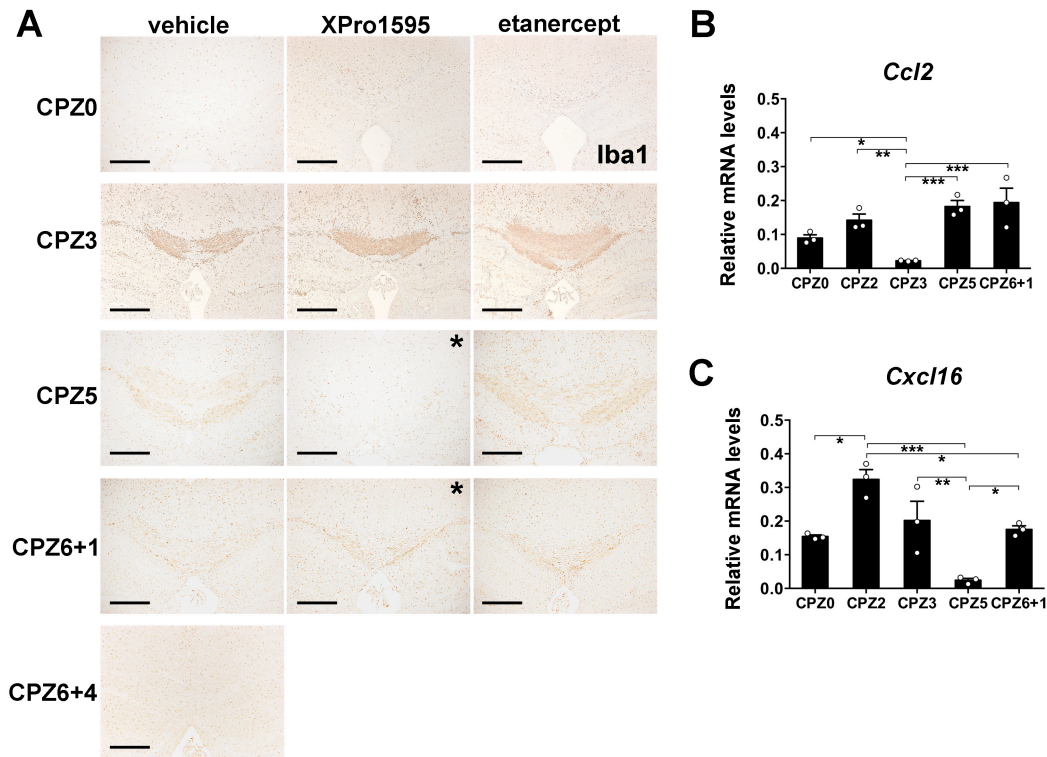
Supplementary Figure 1. Therapeutic inhibition of brain soluble TNF does not alter cuprizone-induced demyelination but promotes myelin recovery. (A) Quantitative representation of 2', 3'-cyclic nucleotide 3'-phosphodiesterase (CNPase) integrated density in the corpus callosum in brain coronal paraffin sections from vehicle-, XPro1595- and etanercept-treated naïve mice (CPZ0) or cuprizone (CPZ)-fed CPZ3, CPZ5 and CPZ6+1 mice (n=8 for vehicle-treated CPZ0, n=4 for XPro1595-treated CPZ0, and n=6-12 for all other time points). (B) Levels of mRNA encoding the myelin structural protein myelin basic protein (MBP) relative to those of *Gusb* in whole brain samples from vehicle-treated CPZ0, CPZ2, CPZ3, CPZ5 and CPZ6+1 mice by quantitative RT-PCR (n=4 per group). The results shown are from one representative of two (B) or three (A) independent experiments. Statistical comparisons between measurements of CNPase integrated density by two-way ANOVA with Bonferroni's test (A), and mRNA levels by ordinary one-way ANOVA with Tukey's test (B), *p<0.05, **p<0.01 (B, C, E). Circles show values for individual mice.



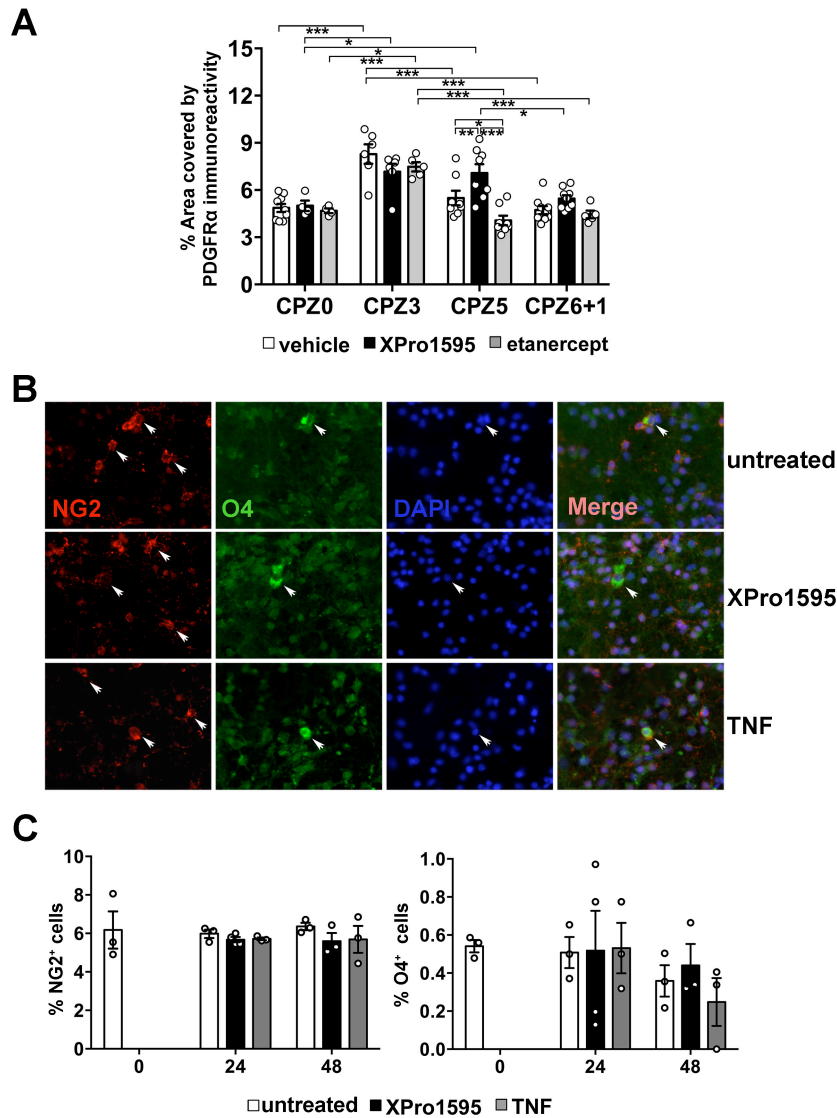
Supplementary Figure 2. Corpus callosum volume increases equally in vehicle- and XPro1595-treated mice during cuprizone demyelination. (A) The total volume of corpus callosum was measured in brain coronal cryostat sections from vehicle- and XPro1595-treated naïve (CPZ0) or cuprizone (CPZ)-fed, CPZ3 and CPZ5 mice. Measurements of demyelination by Klüver-Barrera Luxol fast blue stain (LFB) from Fig. 1B (B), and areas covered by neurofilament H non phosphorylated SMI 32 immunoreactivity from Fig. 2B (C), Glial fibrillary acidic protein (GFAP)- immunoreactivity (D), and numbers of platelet- derived growth factor receptor alpha (PDGFRα)-immunoreactive cells from Fig. 4B (E), were normalized to incorporate the total corpus callosum volume at CPZ0, CPZ3 and CPZ5 time points. The results shown are from one (D) representative of two (E) or three (B, C) independent experiments. Statistical comparisons between measurements by two-way ANOVA with Bonferroni's test, * $p < 0.05$, ** $p < 0.01$, *** $p < 0.001$. Circles show values for individual mice.



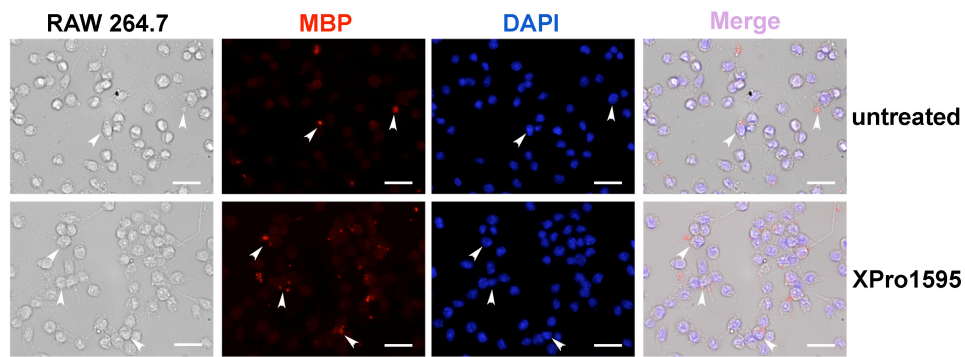
Supplementary Figure 3. Peripherally administered XPro1595, but not etanercept, reaches brain tissues in cuprizone-treated mice. (A, B) Levels of human TNF (XPro1595) and human TNF receptor 2 (etanercept) were measured in serum (A) and PBS-perfused brain homogenates (B) from cuprizone (CPZ)-treated mice that were treated with vehicle, XPro1595 or etanercept for 3 weeks prior to sacrifice at CPZ5 (6 injections) (n=5 per group), using immunoassays specific for human TNF or human TNF receptor 2, that do not cross-react with mouse TNF or mouse TNF receptor 2, respectively.



Supplementary Figure 4. Inhibition of brain soluble TNF promotes early resolution of microgliosis in demyelinated lesions. (A) Ionized calcium binding adaptor molecule 1 (Iba1) immunostaining of microglia in brain coronal paraffin sections of corpus callosum from representative vehicle- (left column) XPro1595- (middle column) and etanercept- (right column) treated CPZ0, CPZ3, CPZ5 CPZ6+1 and CPZ6+4 mice from groups quantitated in Fig. 3B (n=8 for vehicle-treated CPZ0, n=4 for XPro1595-treated CPZ0, and n=6-12 for all other time points). Scale bars 500μM. Asterisks denote early resolution of microgliosis. (B) Levels of mRNA encoding the chemokines chemokine (C-C motif) ligand 2/ monocyte chemoattractant protein 1 (*Ccl2*) and chemokine (C-X-C motif) ligand 16 (*Cxcl16*), relative to those of *Gusb*, in whole brain samples of vehicle-treated CPZ0, CPZ2, CPZ3, CPZ5 and CPZ6+1 mice by quantitative RT-PCR (n=4 per group). The results shown are from one representative of two (B, C) or three (A) independent experiments. Statistical comparisons between measurements of mRNA levels by ordinary one-way ANOVA with Tukey's test (B, C), *p<0.05, **p<0.01, ***p<0.001. Circles show values for individual mice.



Supplementary Figure 5. Soluble TNF does not alter OPC differentiation in mixed neuron-glial cultures. (A) Quantification of area covered by platelet-derived growth factor receptor alpha (PDGFR α)-immunoreactivity in coronal paraffin sections of corpus callosum from vehicle-, XPro1595- and etanercept-treated CPZ0, CPZ3, CPZ5 and CPZ6+1 mice (n=8 for vehicle-treated CPZ0, n=4 for XPro1595-treated CPZ0, and n=6-12 for other time points). (B) NG2 chondroitin sulphate proteoglycan (NG2) immunostaining of oligodendrocyte progenitor cells (OPC) (red), O4 immunostaining of oligodendrocytes (OLG) (green) and DAPI nuclear counterstain (blue) in mixed cortical neuron-glial cultures after 48h treatment with medium (upper row), XPro1595 (middle row), or murine recombinant TNF (lower row). (C) Proportions of NG2- (left graph) and O4-positive cells (right graph), compared to total DAPI-stained cells in cultures after 24 and 48 h with the various treatments. Statistical comparisons between measurements by two-way ANOVA with Bonferroni's test, *p<0.05, **p<0.01, ***p<0.001. Circles show values for individual mice.



Supplementary Figure 6. Inhibition of solTNF increases myelin phagocytosis by murine macrophage cells. Representative photomicrographs of myelin basic protein (MBP) immunostained myelin-containing macrophages (red) with DAPI nuclear counterstain (blue) in cultures of RAW264.7 murine macrophage cells grown on myelin in the presence of medium or XPro1595 (100 ng/ml) for 40 h, as quantitated in Fig. 7E. Scale bar 20 μ M.